Available online at www.sciencedirect.com
ScienceDirect
Continental Shelf Research 27 (2007) 1249–1263
CONTINENTAL SHELF RESEARCH
www.elsevier.com/locate/csr

# Hurricane-induced motions and interaction with ocean currents

L.-Y. Oey[a,*], T. Ezer[a,1], D.-P. Wang[b], X.-Q. Yin[a], S.-J. Fan[c]

[a]*Princeton University, USA*
[b]*State University of New York, @ Stony Brook USA*
[c]*Stevens Institute of Technology, USA*

Received 3 February 2006; received in revised form 8 September 2006; accepted 18 September 2006
Available online 30 January 2007

**Abstract**

Hurricanes produce mixing and flow divergences (and convergences) that alter the upper-ocean heat content (*OHC*), which in turn affects the storm. Ocean observations under a hurricane are rare, making it difficult to validate forecast models. Past research have mainly focused on *OHC*-changes by vertical mixing and tacitly assumed that horizontal transports are slowly varying. Moreover, effects of coastal boundaries on ocean responses to hurricanes are generally omitted. This work uses satellite data to detect and verify forecast isopycnal motions under hurricane Wilma (Oct/16–26/2005) in the Caribbean Sea and the Gulf of Mexico. The model is then used to show that Wilma-induced convergences in northwestern Caribbean Sea produce increased Yucatan-Channel transport into the Gulf ahead of the storm, and the Yucatan–Loop Current front diverts most of this heat around the Loop. This response is distinct from that of an ocean without the Loop, for which warming is widespread north of the channel. These intricate ocean responses can impact hurricane predictions.


*Keywords:* Hurricanes; Surface water waves; Surface temperature; Ocean circulation; Satellite altimetry data; Loop current

## 1. Introduction

The ocean is vital to a more complete understanding of the genesis and evolution of intense tropical storms because of its capacity to store, transport and release heat (hurricanes in the Atlantic and typhoons in the Pacific). An excellent account of the subject is given in Emanuel (2005a). Over the North Atlantic Ocean, the so-called "African easterly waves" which are generated by an instability of the African easterly jet are now believed to serve as the "seedling" circulations for a large proportion of tropical cyclones there (Burpee, 1972). Nearly 85% of the intense hurricanes (Saffir-Simpson Scale Categories 4 and 5) have their origins as easterly waves (Landsea, 1993). Amongst the various necessary conditions for the development of tropical cyclones (e.g. Emanuel, 2005a), an important one is the existence of warm ocean surface (warmer than approximately 26 °C throughout a sufficient depth ≈ 50–100 m) that provides the fuel for the heat engine of the storm.

The 2005 Atlantic hurricane season with three Category-5 hurricanes (Katrina, Rita and Wilma; see Fig. 1(a) and http://www.nhc.noaa.gov/pastall.shtml) in the Caribbean Sea and the Gulf of Mexico underscored an important fact: as populations boom

*Corresponding author. Tel.: +1 609 258 5971; fax: +1 609 258 2850.
*E-mail address:* lyo@princeton.edu (L.-Y. Oey).
[1]Now at: Old Dominion University, USA.

0278-4343/$ - see front matter © 2007 Elsevier Ltd. All rights reserved.
doi:10.1016/j.csr.2007.01.008

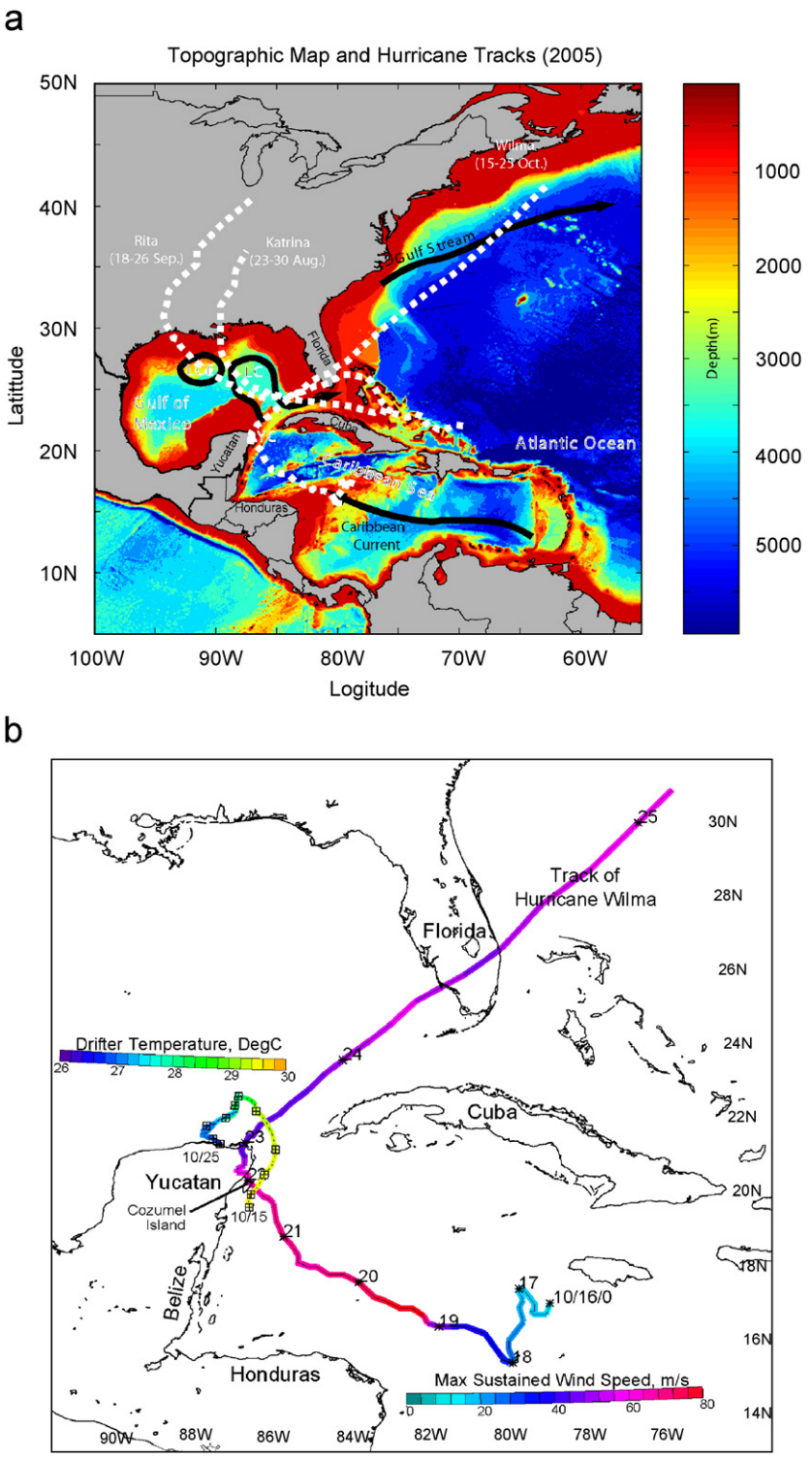


Fig. 1. (a) Topographic map of the western North Atlantic (excluding the Pacific Ocean in the south-west corner, this is the area covered by our ocean forecast model, see text for details). The major ocean currents are indicated by heavy black arrows. The tracks of the three strongest hurricanes in 2005 are indicated in dashed white lines; all three reached a category 5 status during their lifespan (Katrina and Rita in the Gulf of Mexico and Wilma in the Caribbean Sea). Acronyms are LC: Loop Current, LCE: Loop Current eddy, and YC: Yucatan Channel. (b) Track of hurricane Wilma colored with the storm's maximum sustained wind speed, and marked daily from Oct/16/0GMT through Oct/25. Around the Yucatan peninsula, the track of a drifter colored by the sea-surface temperature that it measured is marked (crossed squares) daily beginning from Oct/15 through Oct/25.

in coastal regions, and as the earth embraces a warmer climate with higher sea-surface temperatures (SST) over the tropical oceans, the next decade may see increasingly more intense storms that pose greater risks than ever before (Emanuel, 2005b); the year 2005 was in fact the warmest on record and unprecedented in the Atlantic in terms of tropical cyclone activity (Shein, 2006). The importance of the upper ocean in hurricane development and intensification was recognized by Leipper and Volgenau (1972) who introduced a quantity called the ocean heat content (*OHC*):

$$OHC = \rho_o C_p \int_{Z_{26}}^{\eta} (T - 26)\,dz, \quad T \geqslant 26\,^{\circ}\mathrm{C}, \tag{1}$$

where $Z_{26}$ ($>0$) is depth of the 26 °C isotherm, $\eta$ = sea-surface height (*SSH*), $\rho_0$ density of sea water and $C_p$ the specific heat of water. *SST*'s in excess of 26 °C are necessary for tropical cyclogenesis (Palmen, 1948; DeMaria and Kaplan, 1994). Regions where $OHC > 60$–$90\,\mathrm{kJ/cm^2}$ have been empirically found to be conducive to storm intensification, and *OHC* is now used as one of several parameters in hurricane prediction schemes (DeMaria et al., 2005).

The *OHC* clearly depends on ocean dynamics. For example, lower *OHC* is generally associated with (vertical) mixing and upwelling that bring cooler water to the near-surface, i.e. both $Z_{26}$ and $T$ decrease (Price, 1981; Bender and Ginis, 2000; Shay et al., 2000). The progression speeds, $U$, of most hurricanes are such that $U/C > 1$, and usually $U/C \gg 1$, where $C$ is the first-mode baroclinic wave speed ($\approx 2.5$ m/s in the Caribbean Sea and the Gulf of Mexico (Chelton et al., 1998)). Such a storm ($U > C$) produces lee waves with large vertical isopycnal movements ($>50$ m; vertical velocity $w \approx \pm 10^{-3}\,\mathrm{m\,s^{-1}}$) in the ocean and storm-induced upwelling and downwelling are confined to the immediate neighborhood of the hurricane eye and behind it (Geisler, 1970; Price, 1981; Gill, 1982; Greatbatch, 1983). Coupled with mixing, the local *SST* variations under the eye (diameters 10–100 km),[2] even a modest $\pm 1$ °C, can mean the difference between a storm that rapidly intensifies and one that quickly decays (Cione and Uhlhorn, 2003; Emanuel, 2005a). Yet, the *SST* cooling patterns under the eye often go undetected since it is the most difficult region of the hurricane to accurately and routinely observe, and hence also to validate models. The first goal of this paper is to use satellite observations to detect isopycnal movements under the eye and in the wake of a hurricane (Wilma), and to verify an ocean forecast.

In the Caribbean Sea and Gulf of Mexico where powerful flows such as the Caribbean-Yucatan Current, the Loop Current and eddies (with diameters as large as 400 km) exist, the *OHC* also depends on advection. (Please refer to Oey et al. (2005a) for a review of these currents.) We have found (Oey et al., 2006), for example, that during hurricane Wilma (Oct/16–25/2005), the *SST* at a buoy around the Loop Current slowly increased ($+0.4$ °C) a few days before the storm arrived, then decreased ($-1$ °C) precipitously when the storm passed by. Oey et al. (2006) suggested that the sudden *SST*-drop could be explained by mixing and offshore advection of cooler shelf water by the storm, and that the pre-storm *SST*-rise was due to an increased influx of warm Caribbean Sea water into the Gulf, forced by hurricane-induced Ekman convergent flows that fed the Yucatan–Loop Current system.[3] The Yucatan–Loop Current system plays a central role in this warming process, which redistributes heat ahead of the storm, and which clearly has implications for hurricane predictions. The second goal of this paper is to further illustrate the warming process through numerical experiments.

Section 2 describes satellite data and the forecast model, Section 3 compares satellite observations with forecast upwelling/downwelling cells, and Section 4 presents model experiments that isolate the roles of Yucatan–Loop Current front on upper ocean heat distributions. This paper focuses on hurricane Wilma (Table 1; Fig. 1(b)), and detailed analyses on hurricanes Katrina and Rita will be reported separately. Section 5 concludes the paper, and discusses future roles of ocean forecasts in improving hurricane predictions.

## 2. Methodology

We use *SSH* anomaly (*SSHA*), objectively analyzed *SSHA* (*OASSHA*) and *SST* (*OASST*) from NOAA (www.aoml.noaa.gov/phod/dataphod),

[2]Hurricane Wilma at its peak on 2005/Oct/19/12GMT had an eye's diameter that shrank to only 4–5 km, a record (http://www.nhc.noaa.gov/pastall.shtml).

[3]Large and powerful hurricanes produce winds that mix and cool upper-ocean waters ahead of the storm, as Oey et al. (2006) also found for buoy measurements in the northwest Caribbean Sea during hurricane Wilma.

Table 1
Hurricane Wilma: notable status

| Day/GMT in Oct/2005 | LON | LAT | Min pressure (mb) | Max wind speed ($m\,s^{-1}$) | Saffir-Simpson Category | Comments |
|---|---|---|---|---|---|---|
| 16/12Z | −79.4 | 17.1 | 1003 | 16 | Tropical Depression | Genesis |
| 18/15Z | −80.6 | 16.5 | 977 | 34 | 1 | Hurricane |
| 19/12Z | −82.8 | 17.2 | 882 | 78 | 5 | Most intense |
| 22/06Z | −87.2 | 20.8 | 935 | 60 | 4 | Yucatan landfall |
| 23/06Z | −86.8 | 21.8 | 962 | 45 | 2 | To Gulf of Mexico |
| 24/03Z | −83.7 | 24.4 | 958 | 51 | 3 | Over Loop Current |
| 24/09Z | −82.4 | 25.5 | 950 | 56 | 3 | Prior to landfall at Florida |

AVISO (www.aviso.oceanobs.com), and US-GODAE (www.usgodae.org) sites. Data before and after Wilma and on three pairs of tracks in close proximity are used to estimate changes (Fig. 2). We calculated differences, $\delta SSHA$ = post-storm minus pre-storm *SSHA*, for each pair and interpolated the values onto a regular latitude grid. We used *OASSHA* maps to estimate errors due to the different positions of the paired tracks and found that these errors are small, so that the changes are dominated by the storm. Using differences eliminates ambiguity associated with the unknown mean especially when comparing with the forecast response. In most cases, though, the storm-induced responses are so strong that using the actual *SSHA* yields very similar results. To verify some of the *SST* results, we have also used NDBC buoy data (http://www.ndbc.noaa.gov/; locations in Fig. 3).

We use the Princeton Regional Ocean Forecast System (PROFS; http://www.aos.princeton.edu/WWWPUBLIC/PROFS/) to forecast ocean states in the Caribbean Sea and the Gulf of Mexico during Wilma (Fig. 1). PROFS is based on the Princeton Ocean Model (POM; Mellor, 2004) and has been tested against observations as well as used for process studies (Oey et al., 2005a, b, where a list of recent publications is also given). The forecast, from Oct/16–Nov/06/2005, was initialized from a nowcast field that has already been assimilated with satellites' *SSHA* data up to Oct/16/2005.[4] The nowcast positions of Loop Current and eddies compare well with AVISO. The original (real-time) forecast used Global Forecast System winds (Caplan et al., 1997), but was rerun for this study using the analyzed winds from the Hurricane Research Division (http://www.aoml.noaa.gov/hrd/) of the

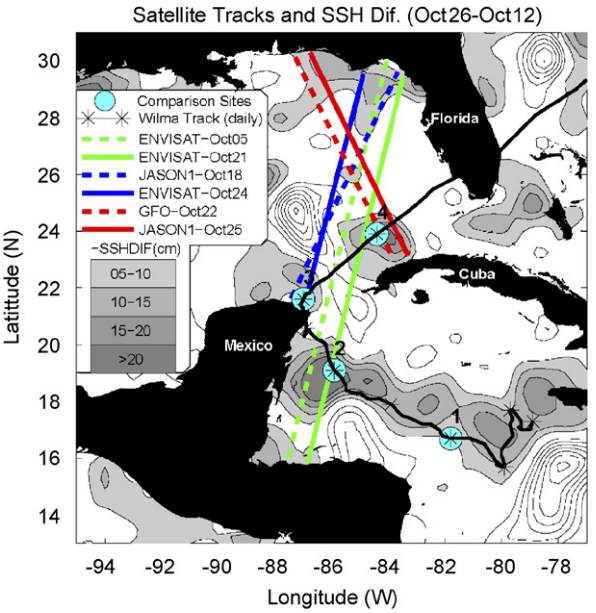


Fig. 2. Contours of difference *OASSHA* (Oct/26 minus Oct/12; contour interval = 5 cm, zero contours omitted), shaded are negative indicating regions of cooling; the inset chart shows contour values. Tracks for the indicated satellites and dates (see inset) are shown; colors indicate pairs of tracks from which differences, $\delta SSHA$, of along-track *SSHA* are shown in Fig. 3. The path of Hurricane Wilma is shown marked daily beginning from Oct/16/2005. Positions of the four sites labeled "1" through "4" at which observed and modeled *SST* and *SSHA* are compared (Fig. 4) are also shown.

National Hurricane Center (NHC).[5] An animation of the wind field can be found at the PROFS website (above). We will still refer to this rerun as "forecast" ("control experiment") to emphasize that it is free from satellite data assimilation. To calculate wind stresses, we use a bulk formula with a high

[4]The nowcast was actually the continuation of a model run that has been assimilated with *SSHA* since 1992.

[5]The timing and intensity for Wilma from all major forecast models were inaccurate especially when the storm was in the Caribbean Sea.

wind-speed limited drag coefficient that fits data for low-to-moderate winds (Large and Pond, 1981) and data for high wind speeds (Powell et al., 2003):

$$\begin{aligned} C_d \times 10^3 &= 1.2, \quad |\boldsymbol{u}_a| \leqslant 11 \text{ m s}^{-1} \\ &= 0.49 + 0.065|\boldsymbol{u}_a|, \quad 11 < |\boldsymbol{u}_a| \leqslant 19 \text{ m s}^{-1}; \\ &= 1.364 + 0.0234|\boldsymbol{u}_a| - 0.00023158|\boldsymbol{u}_a|^2, \\ &\quad 19 < |\boldsymbol{u}_a| \leqslant 100 \text{ m s}^{-1}; \end{aligned} \tag{2}$$

where $|\boldsymbol{u}_a|$ is the wind speed.[6] According to this formula, $C_d$ is constant at low winds, is linearly increasing for moderate winds, reaches a broad maximum for hurricane-force winds, $|\boldsymbol{u}_a| \approx 30$–$50$ m s$^{-1}$, and then decreases slightly for extreme winds. Donelan et al. (2004) suggest that the $C_d$-leveling at high wind may be caused by flow separation from steep waves. Moon et al. (2004) found that $C_d$ decreases for younger waves that predominate in hurricane-forced wave fields. Bye and Jenkins (2006) attribute the broad $C_d$-maximum to the effect of spray, which flattens the sea surface by transferring energy to longer wavelengths.

Surface heat and evaporative fluxes are set to zero so that the *SST* variations are due to model's internal dynamics; Price (1981) found that surface cooling by these fluxes is small compared to cooling by mixing. Bender and Ginis (2000) also used POM for the ocean component of the GFDL coupled model. The main difference is that they initialized using climatology for a spin-up time of O(months). Their initial ocean field therefore never reached an equilibrium state; it did not have a developed Loop Current, eddy-shedding and rings (Hurlburt and Thompson, 1980; Oey, 1996).

The model horizontal grid-size is variable and averages about 10 km in the Loop Current and northwestern Caribbean Sea. There are 25 *sigma layers* with 10 of them in the top 250 m for local water depth ≈2500 m. The Mellor and Yamada's (1982) turbulence closure scheme modified by Craig and Banner (1994) to effect wave-enhanced turbulence near the surface is used. To account for mixing in stable stratification (e.g. internal waves; MacKinnon and Gregg, 2003), Mellor's (2001) modification of a Ridchardson-number-dependent dissipation is used.

[6]This same formula was used in Oey et al. (2006), except that the coefficient for $|\boldsymbol{u}_a|^2$ was erroneously rounded off to 0.0002 at press.

## 3. Satellite observations and forecast

Except for special field programs (e.g. Price, 1981), survey of the upper ocean during a hurricane is not only costly but may also be impractical. One can use *OASSH* before a hurricane and assume that the ocean changes slowly (Shay et al., 2000). However, an active (time-varying) upper ocean is clearly essential in hurricane predictions (Bender and Ginis, 2000). Along-track altimeter data offers near-instantaneous and high resolution (≈5 km) *SSHA* during a hurricane; it has been used in other oceanographic applications in which rapid observations of the sea-surface are required (e.g. in *Tsunami* detection, Geist et al., 2006). However, overlap of satellite tracks and the hurricane path is infrequent. An alternative is to use models. Here we validate forecast's upwelling and downwelling cells under hurricane Wilma by comparing the forecast positions and timings of these cells and the corresponding *SSHA*'s against along-track satellite data.

With a minimum surface pressure of 882 mb and maximum sustained wind speed of around 78 m s$^{-1}$ (Table 1; Fig. 1b), hurricane Wilma was on record the most powerful Atlantic hurricane. The storm formed southwest of Jamaica near a warm eddy with high *OHC*; it strengthened on Oct/18/15*Z* ($|\boldsymbol{u}_a| \approx 34$ m s$^{-1}$) and became a category-5 hurricane on Oct/19/09*Z* as it moved west/northwestward into the Cayman Sea. Wilma weakened as it made landfall on Oct/22/06*Z* at Cozumel Island and Yucatan peninsula, but $|\boldsymbol{u}_a|$ was still > 60 m s$^{-1}$. It weakened further ($|\boldsymbol{u}_a| \approx 45$ m s$^{-1}$) while it moved slowly overland, and strengthened some 24–30 h later ($|\boldsymbol{u}_a| \approx 51$–$56$ m s$^{-1}$ on Oct/24) as it passed over the warm Loop Current and made landfall at Florida.

Wilma is one of the few major hurricanes to directly hit the Yucatan Channel (http://www.nhc.noaa.gov/pastall.shtml), and is also the only such hurricane to have remained in the northwestern Cayman Sea (west of 79 °W) and the Yucatan Channel for a long 7-day period. In the Caribbean Sea, Wilma traveled west/northwestward at $U \approx 2.5$–$3$ m s$^{-1}$, so the averaged $U/C \approx 1.1$. The storm was fast enough to produce lee waves, yet sufficiently slow that the combined action of upwelling and mixing was effective in cooling the near-surface waters (Price, 1981). Theory (Gill, 1982) gives a dominant (lee) wavelength $\lambda_F = (2\pi U/f)[1-(C/U)^2]^{1/2} \approx 160$ km, a frequency $\omega = f/[1-(C/U)^2]^{1/2} \approx 2f$ (period ≈1 day at 18°N), and

a

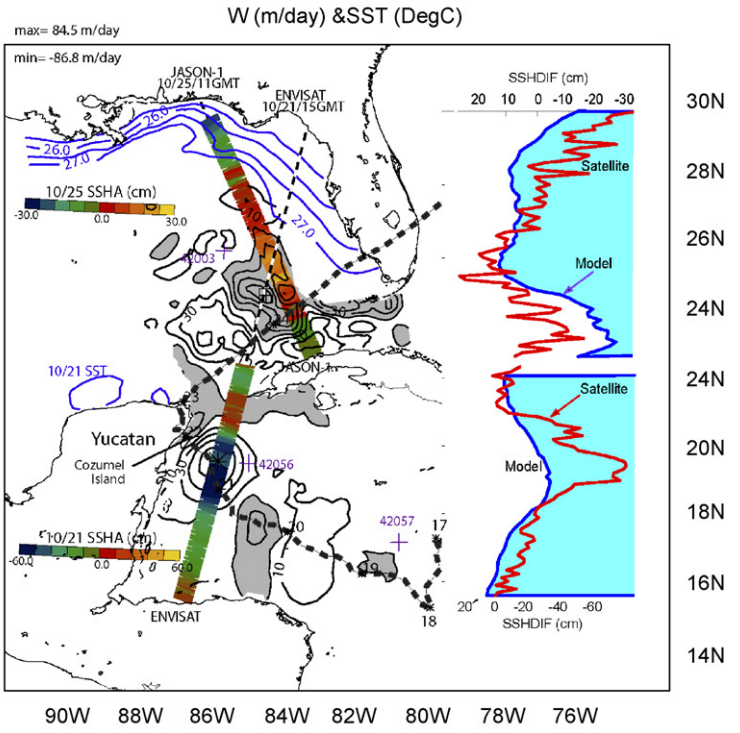
W (m/day) &SST (DegC)
max= 84.5 m/day
min= -86.8 m/day
JASON-1
10/25/11GMT
ENVISAT
10/21/15GMT
SSHDIF (cm)
20 10 0 -10 -20 -30
Satellite
Model
10/25 SSHA (cm)
-30.0 0.0 30.0
26.0
27.0
42003
10/21 SST
JASON-1
Yucatan
Cozumel
Island
42056
42057
10/21 SSHA (cm)
-60.0 0.0 60.0
ENVISAT
Satellite
Model
20 0 -20 -40 -60
SSHDIF (cm)
30N
28N
26N
24N
24N
20N
18N
16N
14N
90W 88W 86W 84W 82W 80W 78W 76W

b

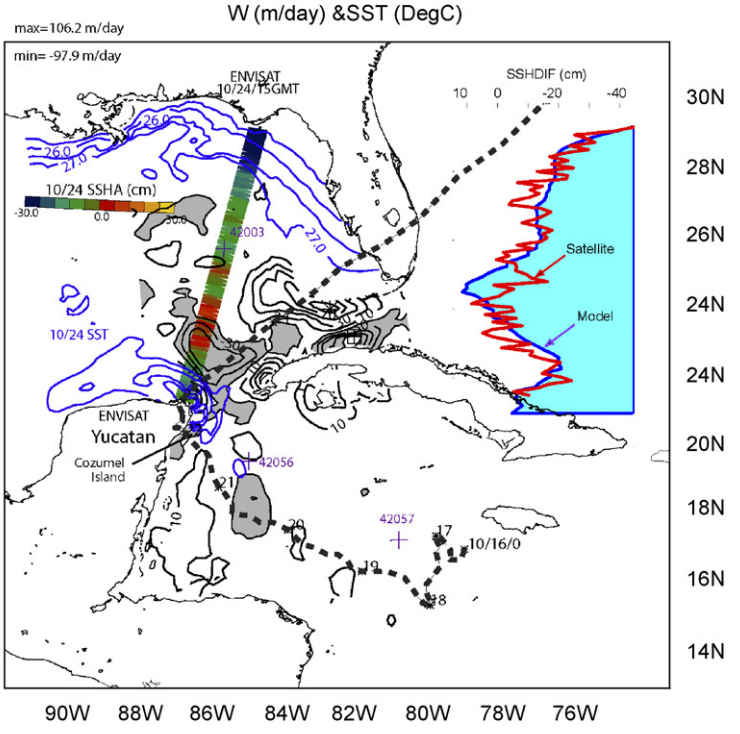
W (m/day) &SST (DegC)
max=106.2 m/day
min= -97.9 m/day
ENVISAT
10/24/15GMT
SSHDIF (cm)
10 0 -20 -40
26.0
27.0
10/24 SSHA (cm)
-30.0 0.0 30.0
42003
Satellite
Model
10/24 SST
ENVISAT
Yucatan
Cozumel
Island
42056
42057
10/16/0
30N
28N
26N
24N
24N
20N
18N
16N
14N
90W 88W 86W 84W 82W 80W 78W 76W

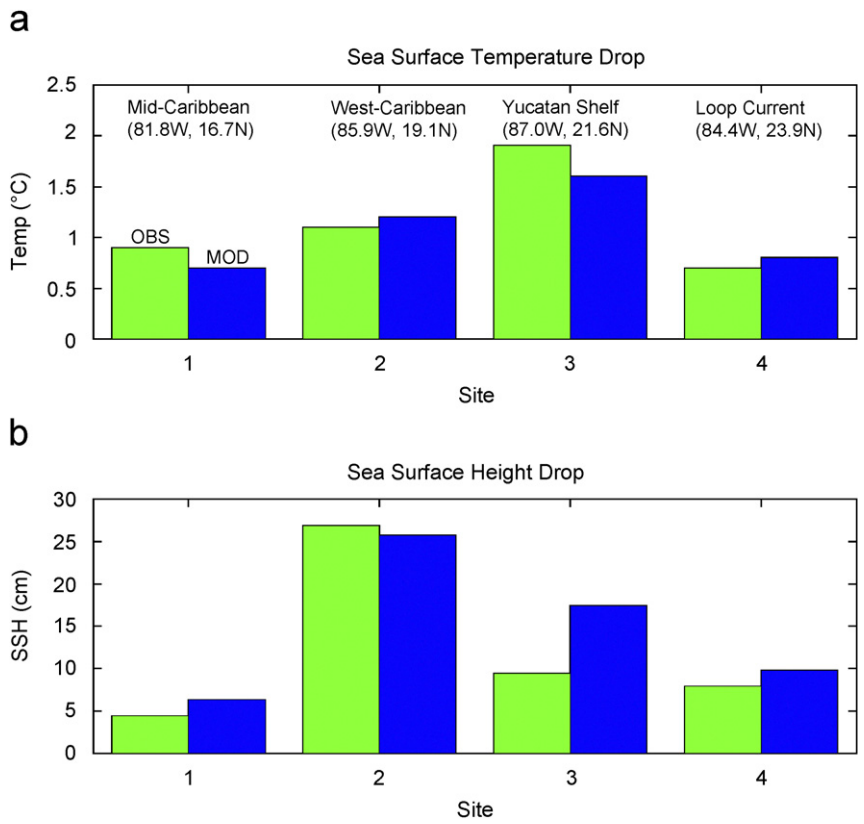


Fig. 4. A comparison of observed (green) and forecast (blue) (a) *SST* and (b) *SSHA* drops (Oct/26 minus Oct/16) at the four sites shown in Fig. 2.

diminished trailing lee-wave amplitudes a fraction ($\approx$0.2–0.3 for $U/C \approx 1.1$) of the main disturbance immediately behind the storm.

Contours of *OASSHA*-difference (Fig. 2), Oct/26 (post-storm) minus Oct/12 (pre-storm), show regions of negative *SSH* indicative of cooling along (and particularly to the right of) the storm in the Caribbean Sea. The rightward cooling bias has traditionally been attributed to the more intense mixing caused by stronger winds to the right of a moving hurricane (i.e. to the right of the storm, wind = hurricane wind + progression speed of the storm; e.g. Price, 1981, and more recently Sheng et al., 2006). This effect exists for Wilma, though it is weaker because the storm moves slowly in the Caribbean Sea. On the other hand, effects of flow convergence to the *left* of the storm due to the presence of the Honduran coast cannot be neglected (see below; Fig. 5). Though the *OASSHA* maps in Fig. 2 are highly smoothed as well as aliased in time, one can still discern a pattern that shows wavelengths of 200–300 km with reduced trailing amplitudes. The wavelength is larger than but not inconsistent with the theoretical estimate. Wilma sped up in the Gulf of Mexico, $U/C \approx 2.3$; theory gives $\lambda_F \approx 560$ km and $\omega \approx f$ (period $\approx 1.23$ day at 24°N). However, while Fig. 2 may contain storm-related signals in the Gulf, the presence of a strong

Fig. 3. (a) Forecast vertical velocity $w$ (black contours, interval = 10 m day$^{-1}$, negative shaded and zero-contour omitted) and *SST* (blue contours, interval = 0.5 °C). Contours south (north) of 22.5 N are for Oct/21/15GMT (Oct/25/11GMT) when Wilma was in the Caribbean Sea (has moved off east Florida). Maximum (minimum) $w$ is indicated by a large asterisk (crossed-square) and values are shown on top-left corner of plot. Superimposed is *ENVISAT* satellite track (south of 22.5 N on Oct/21/15GMT) colored with $\delta SSHA$ = (post-storm minus pre-storm *SSHA*; color-bar shown left of track). A similar track north of 22.5 N is for the *JASON-1* satellite on Oct/25/11GMT (color-bar shown left of track). Wilma's path is shown; numbers on the path indicate days in October/2005. The insets on the right compare forecast and satellite $\delta SSHA$'s along the tracks. (b) Same as (a) but for forecast $w$, *SST* and $\delta SSHA$, as well as for *ENVISAT*'s $\delta SSHA$ on Oct/24/15GMT.

Loop Current and continental shelves makes it difficult to interpret the results based solely on *OASSHA* maps.

Fig. 3 shows the along-track $\delta SSHA$ superimposed on forecast vertical velocity $w$-contours (chosen at $z=-100$ m near the base of the mixed layer, following Price (1981)). We also plot *SST* contours to show cooling over the northern Yucatan shelf during the 4-day period from Oct/21 (Fig. 3a) to Oct/24 (Fig. 3b). Low (high) $\delta SSHA$'s colored as green-blue (red-yellow) generally coincide with upwelling (downwelling, shaded) cells. Prominent ones are: (i) an upwelling cell southeast of Cozumel Island on Oct/21/15*GMT*, a few hours after the storm center has passed: $\delta SSHA\approx -0.7$ m and $w\approx 84\,\mathrm{m\,day^{-1}}$ ($10^{-3}\,\mathrm{m\,s^{-1}}$; Fig. 3a); (ii) a downwelling cell off southwestern Florida slope on Oct/25/11GMT, more than 1 day after the storm: $\delta SSHA\approx 0.2$ m and $w\approx -87\,\mathrm{m\,day^{-1}}$, and also for the same date a smaller upwelling cell north of Cuba where $\delta SSHA\approx -0.2$ m and $w\approx 50\,\mathrm{m\,day^{-1}}$ (Fig. 3a); and (iii) on Oct/24/15GMT (Fig. 3b), an upwelling cell of cooled water off Yucatan where on the shelf $\delta SST\approx -1.5\,^{\circ}\mathrm{C}$ (cf. the *SST*'s of Figs. 3a and b) and $\delta SSHA\approx -0.15$ m, and also a downwelling cell further northeast with $\delta SSHA\approx 0.05$ m and $w\approx -50\,\mathrm{m\,day^{-1}}$.[7] The 1.5 °C drop in *SST* on Yucatan shelf is in excellent agreement with the *SST* measured by a drifter released during Wilma (from the NOAA site www.aoml.noaa.gov/phod/dataphod), shown in Fig. 1b. The drifter recorded an $SST=28.9\,^{\circ}\mathrm{C}$ going northward in the Yucatan Channel on Oct/18/12GMT, and an $SST=27.1\,^{\circ}\mathrm{C}$ as it made a cyclonic turn onto the Yucatan shelf on Oct/23. Note that on the latter two dates (Oct/24/15GMT and 25) shown in Fig. 3, even though the storm has passed, strong ocean responses remain under the Loop Current. Fig. 3 also compares model and satellite $\delta SSHA$s; these generally support the conclusions obtained from the $w$-plots in the ocean's interior. The agreements are better than expected considering the fast nature of the response involving rapidly propagating surface waves. Both observation and model also indicate low sea-levels along the northeastern Gulf coast following Wilma's landfall at southern Florida on Oct/24/10GMT. We do not know the source for the discrepancy between the intensities of observed and modeled minima off the Cozumel Island on Oct/21/15GMT (Fig. 3a). A closer examination of AVISO's *OASSH* maps before Wilma did show a small (diameter $\approx 100$ km) cyclone east of Yucatan. The cyclone was not resolved by the model and may have accentuated the observed *SSH*-drop due to Wilma. The modeled $-0.35$ m drop in this case actually agrees well with the smoothed *OASSH* map (see Fig. 4 at site #2), and corresponds to an isopycnal uplift of about $+60$ m (not shown).

The $w$-contours in the Caribbean Sea (Fig. 3a) show lee waves with amplitudes a fraction ($\approx 1/3$) of the main peak southeast of Cozumel Island and wavelengths $\approx 180$–200 km consistent with the theoretical estimates and also with the *OASSHA* map of Fig. 2. There is a discrepancy between the forecast oscillatory period of about 1.2 day (not shown) and the theoretical estimate of 1 day. However, the longer period may be caused by Doppler shift of the frequency by the westward currents $u$ observed along the southern slope of the Cayman Sea (Fratantoni, 2001). The effective frequency $=(U+u)2\pi/\lambda_F$; substituting a period of 1.2 day gives $u\approx -0.4\,\mathrm{m\,s^{-1}}$, which agrees with the observed speeds of the westward currents in this region.

Fig. 4 compares model and observed drops in *SST* and *SSHA* at four locations along the storm's track as indicated in Fig. 2. The largest drop in *SSHA* is at "site 2" indicating large upwelling (cf. Fig. 3) but because of deep mixed layer in the Caribbean Sea the corresponding *SST* drop is less than that over the Yucatan shelf ("site 3"). Similarly, smaller *SST* drops are seen at "site 1" (mid-Caribbean) and "site 4" (Loop Current). At "site 3" model and observed *SST*-drops compare well suggesting that (since model surface flux $=0$) the predominant shelf cooling is due to upwelling from the upper slope, as seen also from the *SST* contours of Fig. 3b and the drifter mentioned above. The 0.7–1.7 °C drop in *SST*'s shown in Fig. 4 reflects a general post-Wilma cooling in the Caribbean Sea and the eastern Gulf of Mexico, as we also confirm (not shown) from *SST* measurements at the three NDBC stations shown in Fig. 2.

## 4. Loop Current and hurricane-induced currents

The Yucatan–Loop Current is a western boundary current that flows along the eastern Yucatan coast into the Gulf of Mexico; its speeds can exceed 2 $\mathrm{m\,s^{-1}}$ near the surface (please see the review and

[7]The variations are clearly hurricane-induced. Much weaker vertical velocities (magnitudes $\approx 30\,\mathrm{m\,day^{-1}}$ and less) are seen in sensitivity experiments we conducted with zero and weak winds.

the extensive list of references in Oey et al., 2005a). Figs. 5a,b show forecast velocities from the control experiment at $z = -1$ m superimposed on color *OHC* images on (a) Oct/20/12GMT when hurricane Wilma was in the Caribbean Sea and (b) Oct/23/6GMT when the storm was about to leave Yucatan towards Florida. Fig. 5a shows that the storm produces surface convergent flows against the northeastern Yucatan coast. Note also flow convergence along the Honduran coast to the left of the storm, mentioned previously in conjunction with the rightward bias of the *OASSHA*-difference field of Fig. 2. In Fig. 5b, the wind has become directed along the Yucatan–Loop Current front.

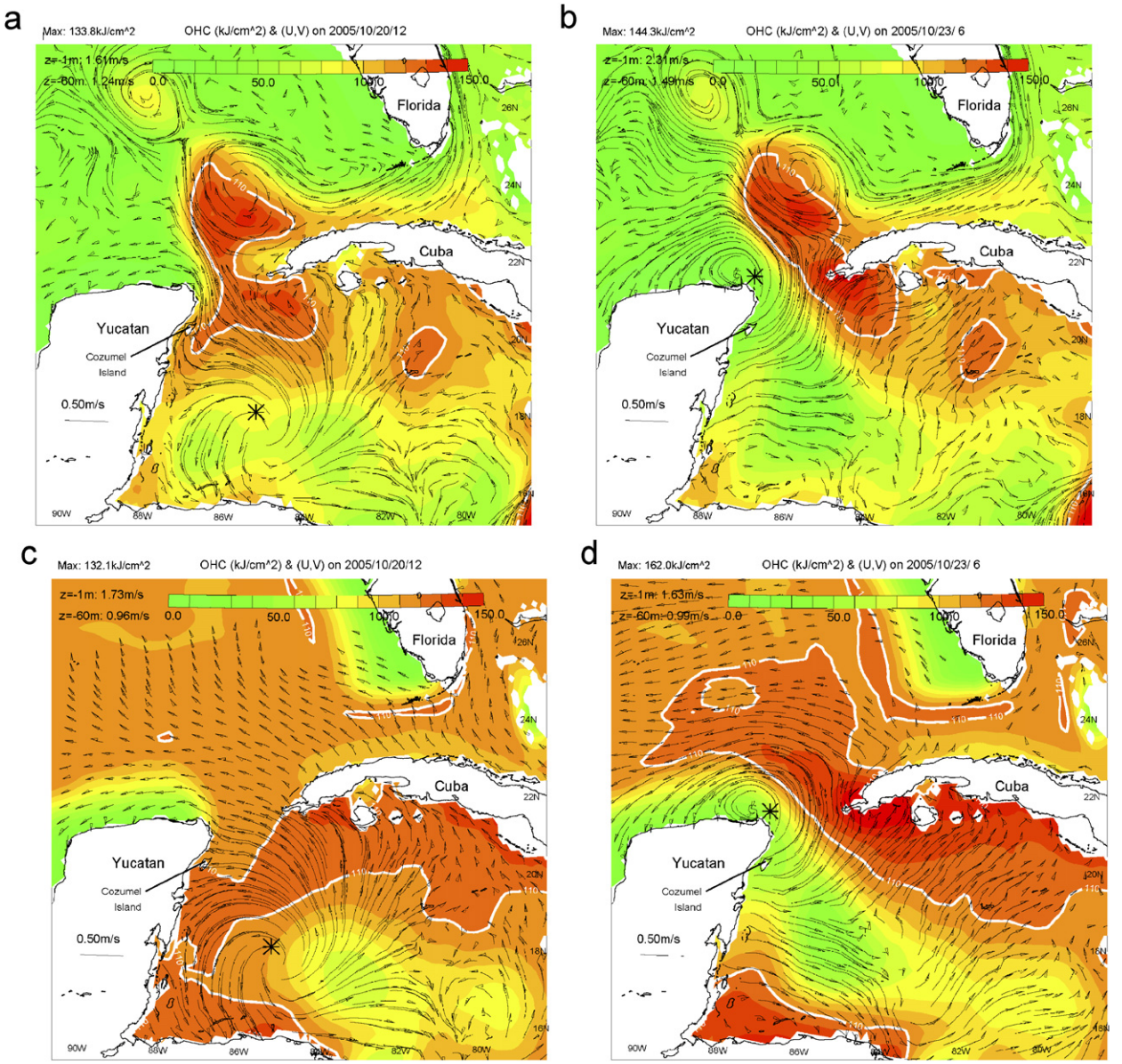


Fig. 5. (a) Color image of the forecast *OHC* on Oct/20/12GMT/2005 during hurricane Wilma. Maximum *OHC* is printed on the top-left corner of the panel. Thick-white contour indicates $OHC = 110\,\mathrm{kJ\,cm^{-2}}$. Forecast currents at $z = -1$ m are shown as black trajectories (with arrows) launched from every other four grid points. Maximum speeds (in Yucatan Channel) at $z = -1$ and $-60$ m are also printed. The large asterisk indicates the position of Wilma at this forecast date. (b) Same as Fig. 5a for Oct/23/6GMT/2005. (c) Same as Fig. 5a (i.e. on Oct/20/12GMT/2005) for the case without the Yucatan–Loop Current frontal system. (d) Same as Fig. 5b (i.e. on Oct/23/6GMT/2005) for the case without the Yucatan–Loop Current frontal system.

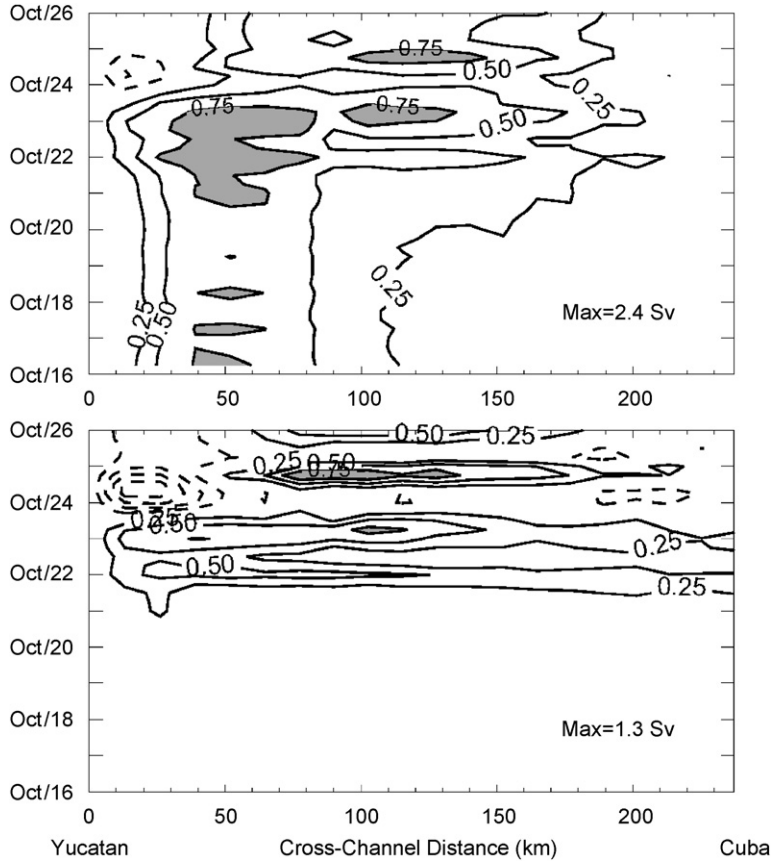


Fig. 6. Transports through the Yucatan Channel in the near-surface 150 m of the model ocean for the control forecast experiment with Loop Current (upper panel) and for the experiment with no Loop Current (i.e. initially level isopycnals; lower panel). These are plotted as a function of cross-channel distance and time. Contours are in 1/4 of the maximum value in $Sv$ ($=10^6\,\mathrm{m\,s^{-3}}$) as indicated in each panel. Zero contour is omitted and shaded are where values $>3/4$ of maximum.

Convergence and down-front wind strengthen oceanic fronts (Wang, 1993; Thomas and Lee, 2005), and Figs. 5a,b show large amount of near-surface currents into the Yucatan Channel.

Is the response fundamentally different if the Yucatan–Loop Current were absent? To address this, we conduct another experiment in which the model ocean is initially at rest with level isopycnals. We choose the vertical temperature and salinity (hence density) profiles to be area averages of the Caribbean Sea's climatology profiles used in the control experiment. The model is then forced by the same Wilma wind field used in the control experiment, and for the same period from Oct/16 through Nov/06/2005. As a check, we repeated the same (level-isopycnal) experiment but without the wind, and confirmed that a trivial solution (zero velocities) was obtained.

Figs. 5c,d show the *OHC* and surface velocities for the level-isopycnal experiment. In addition to cooling (indicated by decreased *OHC*) along the hurricane's path, the figures clearly show regions of increased *OHC* due to convergent (downwelling) flows onto coastlines: southern Cuba and also

Fig. 7. (a) Color image of the temperature-difference between experiments with and without hurricane Wilma for the control experiment at $z=-50$ m on Oct/23/06GMT. This shows Wilma-induced warming around the Loop Current, and cooling along Wilma's path in the Caribbean Sea. The path of Wilma is shown colored with its corresponding maximum sustained wind speeds (color-scale at bottom). Numbers next to small asterisks indicate days in October/2005, and Wilma's position on Oct/23/06GMT is marked. (b) Same as Fig. 7a but for the initially level isopycnal experiment (i.e. without the Loop Current). In contrast to Fig. 7a, this now shows the spread of warm water north of the Yucatan Channel from the Caribbean Sea into the Gulf of Mexico, though cooling along Wilma's path in the Caribbean Sea still exists.

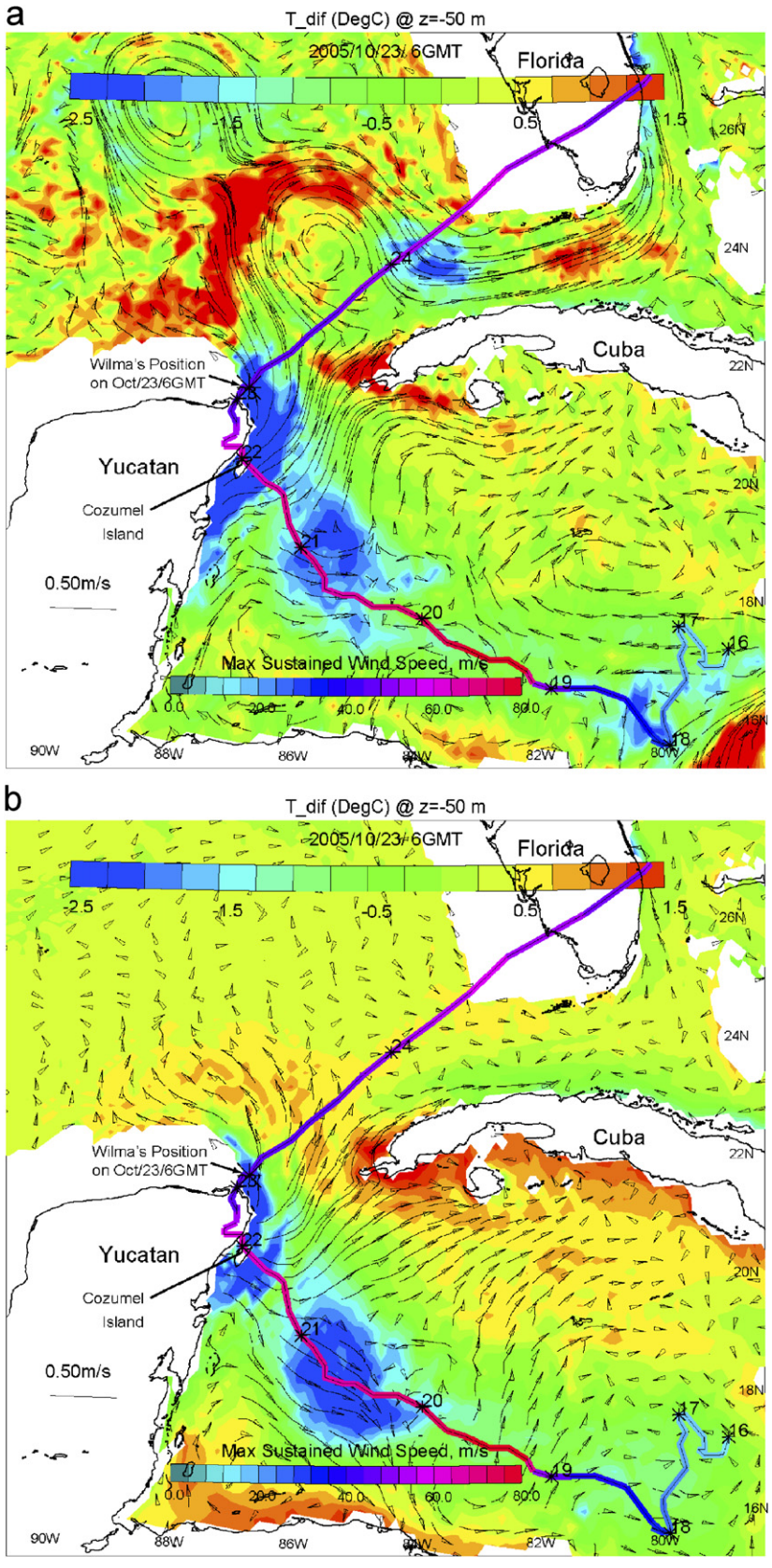
a
T_dif (DegC) @ z=-50 m
2005/10/23/ 6GMT
Florida
-2.5
-1.5
-0.5
0.5
1.5
26N
24N
Cuba
22N
Wilma's Position
on Oct/23/6GMT
Yucatan
20N
Cozumel
Island
0.50m/s
18N
Max Sustained Wind Speed, m/s
0.0
20.0
40.0
60.0
80.0
16N
90W
88W
86W
84W
82W
80W
b
T_dif (DegC) @ z=-50 m
2005/10/23/ 6GMT
Florida
-2.5
-1.5
-0.5
0.5
1.5
26N
24N
Cuba
22N
Wilma's Position
on Oct/23/6GMT
Yucatan
20N
Cozumel
Island
0.50m/s
18N
Max Sustained Wind Speed, m/s
0.0
20.0
40.0
60.0
80.0
16N
90W
88W
86W
84W
82W
80W

northeastern Yucatan (for Fig. 5c). There are also increased flows into the Yucatan Channel, but they are spread across the channel. By contrast, for the control experiment (Figs. 5a,b), the surface flows tend to concentrate along the Yucatan–Loop Current front. Fig. 6 compares near-surface 150 m transports through the Yucatan Channel for the control and level-isopycnal experiments. Intensification of the western-boundary jet in the control experiment begins around Oct/20–21, while the level-isopycnal experiment shows broader increased flows that extend to the mid-channel. The broad flows result in a correspondingly broad increase in *OHC* north of the channel (compare Figs. 5c and d). By contrast, Oey et al. (2006) show that, in the control experiment, the heat input through the channel is concentrated around the Loop, contributing to a temperature increase of about 1 °C.[8] The corresponding increase in *OHC* around the Loop is barely discernible in Fig. 5. However, the increase is clearly seen by taking differences (in either temperature or *OHC*) between the experiment with wind (i.e. control or level-isopycnal) and a corresponding experiment without wind. Taking differences in this way minimizes contributions from background variability that is not related to hurricane Wilma especially for the control experiment. However, we obtain very similar results by simply subtracting the initial conditions. Fig. 7 shows the difference-temperatures at $z = -50$ m for (a) the control and (b) level-isopycnal experiments.[9] In (b) the warm water spreads into the Gulf, while in (a) it is concentrated along the Loop and has about three-time higher temperatures (1.5 °C rise instead of 0.5 °C).

Strong flows such as the Loop Current therefore impact the distribution of heat and cannot be neglected in hurricane predictions. In the case of hurricane Wilma, the heat redistribution (by the Loop) may have had some practical significance. In the absence of the Loop the storm would have traversed over a larger area of high *OHC* on its way to Florida; in other words, Wilma would have traversed over the pool of warmer water that it forced through the channel into the Gulf (Figs. 5c,d)! The Loop diverted this warm water "out of Wilma's way," so to speak. To further illustrate this finding, we average *OHC* (and other variables) over circles of radii 50 km centered at the hurricane's track over its lifespan. This results in along-track and time (two-dimensional) arrays for each variable. The assumption is that, as far as the storm is concerned, the ocean surface directly under the eye is the most relevant (Emanuel, 2005a). Fig. 8 plots the *OHC*-difference (i.e. track values on Oct/16 are subtracted) contours for (a) the control experiment and (b) the initially level isopycnal experiment. In general, cooling occurs when the storm comes near or after it has passed (i.e. solid contours which indicate cooling are above the storm's track in the figure). Notable exceptions occurred in Fig. 8a for the control experiment over the Yucatan shelf (along-track distance $\approx 1600$ km; cf. Fig. 4a, site3) and also over the Loop Current's southern core just north of the Yucatan Channel (along-track distance $\approx 1900$ km) where *OHC*-drop of as much as $-30\,\mathrm{kJ\,cm^{-2}}$ occurred a few days before the storm actually arrived. The cooling is caused by wind-induced vertical mixing and westward Ekman currents towards the Yucatan–Loop Current front. By contrast, despite a similar cooling in the absence of the Loop Current, Fig. 8b actually shows a slight warming because of the presence of the pool of warmer water just north of the channel (Figs. 5d and 7b).

## 5. Conclusion

We emphasize that the model isopycnal motions as indicated by the *w*-contours and *SSHA*'s in Fig. 3 are forecast results (i.e. not assimilated with satellite *SSHA*). We have shown, therefore, that along-track satellite altimeter data is useful for evaluating forecast skills of an ocean model during a hurricane. Assuming an accurate wind field, the generally good agreements between model and observation in terms

Fig. 8. Along-hurricane-track and time contours of *OHC*-difference (i.e. the initial along-track values have been subtracted) in $\mathrm{kJ\,cm^{-2}}$ for (a) the control experiment (with Loop Current) and (b) the initially level isopycnal experiment (without Loop Current). Hurricane Wilma track (colored with its maximum sustained wind speed, scale shown) is also shown on this distance–time space, so that the slope is equal the inverse of the storm's progression speed. Negative contours (i.e. cooling) are solid and shaded, positive (i.e. warming) are dashes and the zero-contour is omitted. The white region above Wilma's track at Yucatan in "(a)" is land.

[8]Another contribution, 20–30%, is due to wind-induced convergence at the Loop Current front.

[9]We choose subsurface (e.g. $z = -50$ m) for comparison because for the level-isopycnal experiment, since surface fluxes = 0 and initially there are no horizontal thermal gradients, warming can only occur below the surface, caused by flow convergences and advection by the storm.

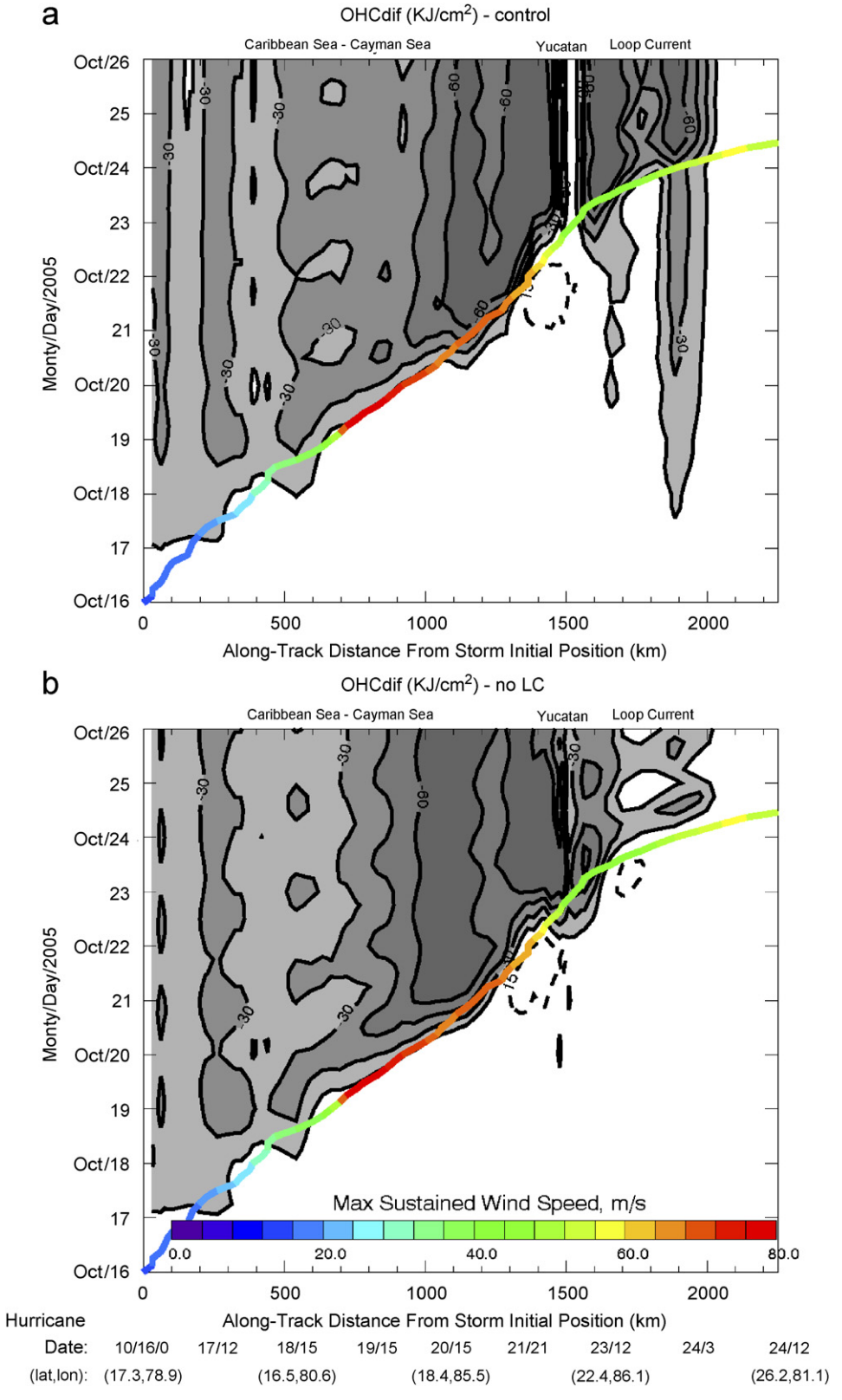
a
OHCdif (KJ/cm2) - control
Caribbean Sea - Cayman Sea
Yucatan
Loop Current
Monty/Day/2005
Oct/26
25
Oct/24
23
Oct/22
21
Oct/20
19
Oct/18
17
Oct/16
0
500
1000
1500
2000
Along-Track Distance From Storm Initial Position (km)
b
OHCdif (KJ/cm2) - no LC
Caribbean Sea - Cayman Sea
Yucatan
Loop Current
Max Sustained Wind Speed, m/s
0.0
20.0
40.0
60.0
80.0
Hurricane
Date:
(lat,lon):
10/16/0
17/12
18/15
19/15
20/15
21/21
23/12
24/3
24/12
(17.3,78.9)
(16.5,80.6)
(18.4,85.5)
(22.4,86.1)
(26.2,81.1)

of the timings and locations of upwelling and downwelling cells are encouraging, and suggest that hurricane-induced vertical motions are deterministic even in a complex mesoscale eddy field (e.g. Loop Current and eddies). We conclude that satellite along-track data offers a high-resolution dataset against which the ocean component of a hurricane forecast system can be routinely validated. The limiting factor is the availability of accurate forecast wind.

On the other hand, the presence of powerful ocean currents and coastal boundaries gives rise to intertwined hurricane-ocean interactions that in turn can modify the storm. In the case of hurricane Wilma, we show that the Yucatan–Loop Current system diverted heat away from the storm's projected path, and may have helped tame the storm before it hit Florida.

Existing hurricane coupled models (e.g. Bender and Ginis, 2000) have simplified ocean-initialization schemes that do not accurately model the Loop Current and eddies. Statistical prediction systems (e.g. DeMaria et al., 2005) in part rely on smoothed *OASSH* maps and assume that the ocean is slowly varying. The present study suggests that future hurricane predictions may benefit from more proactive ocean forecasts that are initialized by data assimilation (e.g. satellite data). An important facet of improved prediction is the inclusion of a more refined parameterization of wind-induced mixing process: effects of surface waves under strong winds in particular. For example, Oey et al. (2006) noted that the *SST* at NDBC 42056 (Fig. 3) began to drop days before the arrival of Wilma; i.e. when the storm was near NDBC 42057. We attributed the cooling to the large size of the storm that produced current mixing from a distance. However, the cooling may also have been additionally induced by mixing due to swells that were generated when Wilma was at its peak intensity hundreds of kilometers to the east.

## Acknowledgments

We are grateful to the Minerals Management Service (MMS) for supports (Contract #1435-01-06-CT-39731). Computing was done at GFDL/NOAA.

## References

Bender, M.A., Ginis, I., 2000. Real-case simulations of hurricane–ocean interaction using a high-resolution coupled model: effects on hurricane intensity. Monthly Weather Review 128, 917–946.

Burpee, R.W., 1972. The origin and structure of easterly waves in the lower troposphere of North Africa. Journal of Atmospheric Science 29, 77–90.

Bye, J.A.T., Jenkins, A.D., 2006. Drag coefficient reduction at very high wind speeds. Journal of Geophysical Research 111 (C3), C03024.

Caplan, P.J., Derber, W., Gemmill, S., Hong, -Y., Pan, H.-L., Parish, D., 1997. Changes to the NCEP operational medium-range forecast model analysis/forecast system. Weather Forecasting 12, 581–594.

Chelton, D.B., DESzoeke, R.A., Schlax, M.G., Naggar, K.E., Siwertz, N., 1998. Geographical variability of the first baroclinic Rossby radius of deformation. Journal of Physics and Oceanography 28, 433–460.

Cione, J.J., Uhlhorn, E., 2003. Sea surface temperature variability in hurricanes: implications with respect to intensity change. Monthly Weather Review 131, 1783–1796.

Craig, P.D., Banner, M.L., 1994. Modeling wave-enhanced turbulence in the ocean surface layer. Journal of Physics and Oceanography 24, 2546–2559.

DeMaria, M., Kaplan, J., 1994. Sea surface temperature and the maximum intensity of Atlantic tropical cyclones. Journal of Climate 7, 1324–1334.

DeMaria, M., Mainelli, M., Shay, L.K., Knaff, J.A., Kaplan, J., 2005. Further improvement to the Statistical Hurricane Intensity Prediction Scheme (SHIPS). Weather Forecast 20, 531.

Donelan, M.A., Haus, B.K., Reul, N., et al., 2004. On the limiting aerodynamic roughness of the ocean in very strong winds. Geophysical Research Letters 31, L18306.

Emanuel, K.A., 2005a. Divine Wind—The History and Science of Hurricanes. Oxford University Press, New York.

Emanuel, K., 2005b. Increasing destructiveness of tropical cyclones over the past 30 years. Nature 436, 686–688.

Fratantoni, D.M., 2001. North Atlantic surface circulation during the 1990s observed with satellite-tracked drifters. Journal of Geophysical Research 106, 22,067–22,093.

Geisler, J.E., 1970. Linear theory of the response of a two-layer ocean to a moving hurricane. Geophysics and Fluid Dynamics 1, 249–272.

Geist, E.L., Titov, V.V., Synolakis, C.E., 2006. Tsunami: wave of change. Scientific American 294, 56–63.

Gill, A.E., 1982. Atmosphere–Ocean Dynamics. Academic Press, New York, 662pp.

Greatbatch, R.J., 1983. On the response of the ocean to a moving storm: the nonlinear dynamics. Journal of Physics and Oceanography 13, 357–367.

Hurlburt, H.E., Thompson, J.D., 1980. A numerical study of Loop Current intrusions and eddy shedding. Journal of Physics and Oceanography 10, 1611–1651.

Landsea, C.W., 1993. A climatology of intense (or major) Atlantic hurricanes. Monthly Weather Review 121, 1703–1713.

Large, W.G., Pond, S., 1981. Open ocean flux measurements in moderate to strong winds. Journal of Physics and Oceanography 11, 324–336.

Leipper, D.F., Volgenau, D., 1972. Hurricane heat potential of the Gulf of Mexico. Journal of Physics and Oceanography 2, 218–224.

MacKinnon, J.A., Gregg, M.C., 2003. Shear and baroclinic energy flux on the summer New England shelf. Journal of Physics and Oceanography 33, 1462–1475.

Mellor, G.L., Yamada, T., 1982. Development of a turbulence closure model for geophysical fluid problems. Review of Geophysics and Space Physics 20, 851–875.

Mellor, G.L., 2001. One-dimensional, ocean surface layer modeling: a problem and a solution. Journal of Physics and Oceanography 31, 790–809.

Mellor, G.L., 2004. User s guide for a three-dimensional, primitive equation, numerical ocean model. Program in Atmospheric and Oceanic Sciences. Princeton University, 42pp.

Moon, I.-J., Ginis, I., Hara, T., 2004. Effect of surface waves on Charnock coefficient under tropical cyclones. Geophysical Research Letters 31, L20302.

Oey, L-Y., 1996. Simulation of mesoscale variability in the Gulf of Mexico. Journal of Physics and Oceanography 26, 145–175.

Oey, L.-Y., Ezer, T., Lee, H.J., 2005a. Loop Current, rings and related circulation in the Gulf of Mexico: a review of numerical models and future challenges. In: Sturges, W., Lugo-Fernandez, A. (Eds.), Circulation in the Gulf of Mexico: Observations and Models, Geophysical Monograph Series, vol. 161, 360pp.

Oey, L.-Y., Ezer, T., Forristall, G., Cooper, C., DiMarco, S., Fan, S., 2005b. An exercise in forecasting loop current and eddy frontal positions in the Gulf of Mexico. Geophysical Research Letters 32, L12611.

Oey, L.-Y., Ezer, T., Wang, D.-P., Fan, S.-J., Yin, X.-Q., 2006. Loop Current warming by Hurricane Wilma. Geophysical Research Letters 33, L08613.

Palmen, E., 1948. On the formation and structure of tropical cyclones. Geophysics 3, 26–38.

Powell, M.D., Vickery, P.J., Reinhold, T., 2003. Reduced drag coefficient for high wind speeds in tropical cyclones. Nature 422, 279–283.

Price, J.F., 1981. Upper Ocean Response to a Hurricane. Journal of Physics and Oceanography 11, 153–175.

Shay, L.K., Goni, G.J., Black, P.G., 2000. Effects of a warm oceanic feature on hurricane Opal. Monthly Weather Review 128, 1366–1383.

Shein, K.A. (Ed.), 2006. State of the Climate in 2005. Special supplement to the Bulletin of the American Meteorological Society, vol. 87, 6 June 2006.

Sheng, J., Zhai, X., Greatbatch, R.J., 2006. Numerical study of the storm-induced circulation on the Scotian Shelf during Hurricane Juan using a nested-grid ocean model. Progress in Oceanography 70, 233–254.

Thomas, L.N., Lee, C.M., 2005. Intensification of oceanic fronts by down-front winds. Journal of Physics and Oceanography 35, 1086–1102.

Wang, D.-P., 1993. Model of frontogenesis: subduction and upwelling. Journal of Marine Research 51, 497–513.